

Innovative Impact Assessment of Electric Vehicles Charging Loads on Distribution Transformers using Real Data

R. Godina^a, E.M.G. Rodrigues^a, N.G. Paterakis^b, O. Erdinc^{c,d},
and J.P.S. Catalão^{a,d,e,*}

^a C-MAST, University of Beira Interior, R. Fonte do Lameiro, Covilhã 6201-001, Portugal

^b Department of Electrical Engineering, Eindhoven University of Technology (TU/e), PO Box 513, 5600 MB Eindhoven, The Netherlands

^c Yildiz Technical University, Davutpasa Campus, Esenler, 34220 Istanbul, Turkey

^d INESC-ID, Instituto Superior Técnico, University of Lisbon, Av. Rovisco Pais, 1, Lisbon 1049-001, Portugal

^e INESC TEC and the Faculty of Engineering of the University of Porto, R. Dr. Roberto Frias, Porto 4200-465, Portugal

Abstract

Widespread adoption of electric vehicles (EVs) could bring social and economic benefits. The effort of promoting the use of EVs in transportation is indispensable to meet the climate change related targets and to reduce the dependency on the ever unstable prices of diminishing fossil fuels. However, there are still many uncertainties in the market regarding the acceptability of EVs by the final consumer. As a new contribution to earlier studies, this paper assesses the impact of EV charging load on the dielectric oil deterioration of two real power distribution transformers (PDT), one residential and one industrial, located in the insular grid of São Miguel Island. A PDT thermal model is used to estimate the hot-spot temperature given the load ratio. Real data are used for the main inputs of the model, namely, the daily residential load curve, the daily private industrial client load curve, the PDT parameters, time-of-use rates and EV parameters.

Keywords: Battery; distribution transformer; EV charging; loss-of-life; transformer ageing.

Nomenclature

V	Relative ageing rate.
d	The daily distance covered by an EV.
d_R	The maximum range of the EV.
μ	The natural logarithmic mean.
σ	The standard deviation of the corresponding normal distribution.
Θ_a	The average ambient temperature in °C.
Θ_h	Winding hottest-spot temperature in °C.
Θ_o	Top-oil temperature in °C.
$\Delta\Theta_{hi}$	Hot-spot-to-top-oil (in tank) gradient at start in K.
$\Delta\Theta_{oi}$	Top-oil (in tank) temperature rise at start in K.
$\Delta\Theta_{or}$	Top-oil temperature rise at rated current in K.
$\Delta\Theta_{hr}$	Hot-spot temperature rise at rated current in K.
R	Ratio of load loss to no-load loss at rated current.
K	Load factor (load current/rated current).
x	Exponential power of total losses versus top-oil (in tank) temperature rise (oil exponent).
y	Exponential power of current versus winding temperature rise (winding exponent).
k_{11}	Thermal model constant.
k_{21}	Thermal model constant.
k_{22}	Thermal model constant.

* Corresponding author at the Faculty of Engineering of the University of Porto, R. Dr. Roberto Frias, 4200-465 Porto, Portugal.
E-mail address: catalao@ubi.pt (J.P.S. Catalão).

τ_o	Average oil time constant.
τ_w	Winding time constant.
H	Hot-spot factor.
E_i	The initial SOC of an EV battery.
g_r	Average winding to average oil (in tank) temperature gradient at rated current in K.
V_n	Relative ageing rate during interval n .
Δt_n	Time interval.
N	Total number of time intervals.
P_{EV}	EV rated charging power in W.
P_d	Domestic loads in W.
P_r	Distribution transformer rated power in W.
P_f	Factory load in W.
P_T	Total load in W.
L	Loss of life.
D	The difference over a small time step.
Dt	Time Step.
t	Period of the day in time units (h or min).

30

31 **Indices**

a	Ambient Temperature
d	Domestic
EV	Electric Vehicle
f	Factory
h	Hot-spot
i	At start/initial
n	Index of the time interval
o	Top-oil
r	Rated Load
t	Period of the day index in time units [h or min].
w	Winding

32

33 **Table of abbreviations**

34

ACAP	Portuguese Automobile Association
DN	Distribution network
EV	Electric vehicle
LOL	Loss of life
ONAN	Oil natural air natural
PDF	Probability density function
PDT	Power distribution transformer
RES	Renewable energy sources
SG	Smart grid
SOC	State of charge

35

36 **1. Introduction**

37

38 Concerns regarding urban air pollution, the climate change, and the dependency on instable and costly
39 supplies of fossil fuels have compelled policy makers and researchers to explore other possibilities to
40 conventional fossil-fuelled internal combustion engine vehicles. One such alternative is the introduction
41 of electric vehicles (EVs) to replace conventional vehicles [1] [2] [3]. The broad adoption of such a
42 means of transportation could signify a drastic reduction in greenhouse gases emissions and a compelling
43 argument for the collective attempts to meet the emission mitigation goals [4] [5] [6]. As a result, during
44 the last few years the electrification of transportation has been increasingly drawing attention.

45 The wide adoption of EVs is more challenging in comparison with the use of conventional and hybrid
46 vehicles since the main energy source is electricity and therefore, the electric power systems should be
47 qualified to accommodate new challenges and take advantage of the opportunities that are associated with
48 the EV recharging load [7]. Moderate penetration levels might have a low impact on the grid.
49 Nevertheless, as the number of EVs increases, a real possibility of the electric power systems being
50 overloaded emerges – especially in the existing distribution network (DN) [8] [9].

51 An event of a large number of EVs charging – if occur simultaneously – can lead to grid inadequacy in
52 terms of security and available network capacity. This situation can be averted in such cases where the
53 EVs are appropriately incorporated into the electric power system. For the EVs point of view, an occasion
54 of a high number of EVs charging at the same time could eventually be realistic [10]. Without a proper
55 assimilation, the electric power system may possibly suffer excessive voltage drops, feeder congestion,
56 etc., especially in the case of an isolated electrical grid, such as the one of São Miguel Island, Azores – a
57 region that lacks a suitable plan for EV integration into the local electric power system.

58 The smart grid (SG) is defined as an electricity network that is capable of integrating in a smart way
59 the actions of all users connected to it, with the intention to successfully distribute secure, economic, and
60 sustainable electricity supplies [11]. The SG eases the accommodation of renewable energy resources
61 (RES) into the present grid with a higher distributed nature to support the mitigation of carbon emissions.
62 The latest progress made by researchers in the SG field has led to the prediction of the connection of
63 distributed RES and EVs to the power network and the various technical challenges that come from this
64 new paradigm. Thus, the overcoming of such obstacles has to be done appropriately [12].

65 Recently, the implementation of SG enabling technologies in insular areas has been increasing rapidly,
66 with the installation of diverse test systems in islands around the world. Even though the interconnected
67 power system structure is deemed to be more rigid as regards to stability, isolated areas which could offer
68 an essential foundation for potential islanding operation requirements could be seen as perfect testing
69 ground for the pre-evaluation of the SG paradigm [13].

70 The traditional DN is mainly designed as a passive network intended to deliver energy to the
71 consumers [14]. Thus, there is the necessity to create and improve new models and methods with the
72 purpose of assessing the impact that high penetration level of EV charging loads could have on the DN.
73 This is also justified since there is a need to make sure that a high penetration of EVs does not overload
74 the grid without reason, which ultimately adds to the existing efforts of reduction of the environmental
75 impact by the human activity. Power distribution transformers (PDTs) are essential DN infrastructure that
76 could suffer unparalleled charging loads due to the EVs. Several researchers investigated such themes,
77 aiming to evaluate if the current existing electricity network and the PDT dielectric oil may resist to the
78 penetration of EVs on a large scale [15] [16] [17] [18] [19] [20]. In [15] the authors focused on
79 identifying PDTs that are most vulnerable in cases of overloading as a result of the implementation of
80 EVs through the employment of a binomial probability model that estimates the probability of a specific
81 PDT to experience overloading. In [16] a study in which the effect of EVs charging on a local residential
82 transformer by means of an Monte Carlo simulation that was utilised to foresee the final state of charge
83 (SOC) of daily driving for a hybrid EV model and an EV model is performed. In [17] a method to assess
84 the effect of EVs charging on overhead PDTs is described, also presenting a novel smart charging
85 algorithm that regulates EVs charging relying on the assessed PDTs temperatures. In another study [18]
86 the way in which high penetration of EVs will influence the development of home energy management
87 and PDT systems with the intention of decreasing the effect of EV battery charging on PDTs by using real
88 load consumption data from Austin, Texas, is assessed. In [19] a model to investigate the effect of large
89 scale penetration rates of additional power to restore the full level of EV battery SOC on the dielectric oil
90 deterioration of PDTs through UK generic low voltage DN model is presented.

91 One of the most common elements that are found in DN is the PDT with an oil-immersed core. The
92 DN of Azores uses almost exclusively oil-immersed PDTs – some of them upgraded very recently [21].
93 In addition to that, PDTs in their existing form are estimated to be the mainstream option for the years to

94 come, due to their reliability and extensive use. Thus, the impact of specific SG practices such as EV
95 charging on PDTs life and performance considerations must be evaluated in detail.

96 The contribution of this study is threefold:

97 • To present a model that allows the evaluation of the effect of EVs charging loads on the
98 dielectric oil deterioration of two real PDTs, one supplying a residential area and the other a
99 private industrial client, which in turn are part of the isolated electrical grid of São Miguel Island,
100 Azores, Portugal.

101 • To utilise a method that takes into account the uncertainty of EV battery charging loads,
102 for instance the variability of the travel habits of the EV user before recharging – recorded in 2011,
103 the battery SOC at the beginning of the charging process and different charging strategies.

104 • The study of a particular case of an island with scenarios of high penetration of EVs and
105 the EV charging at work during 3 different shifts considering an industrial load.

106 The remainder of the paper is organized as follows: in Section 2, the employed methodology is
107 elaborated. In Section 3, the DN of São Miguel, Azores is presented and two cases are studied, one
108 assessing the impact of EVs charging through the PDT of a residential area and another concerning an
109 industrial client. Simulation results are also provided and discussed. Finally, conclusions are drawn in
110 Section 4.

111

112 **2. Methodology**

113 *2.1 EV battery charging profiles*

114 The charging of EVs is an addition to the existing load. EVs are noticeably distinct when compared to
115 other electrical loads, as a result of their highly mobile and unpredictable nature. Currently, three key
116 factors that could affect the influence of EVs on DN exist, namely, the unique nature of the EV charging
117 process, the driving profile and electrical energy tariff incentives.

118 With the growth of the EV market more and more car manufacturers enter the competition. Hence, a
119 large number of EV types with different characteristics are available today [22]. As a result, in order to be
120 more realistic, five different types of EVs are used in this study. The latest models of real EVs were used
121 in this study – BMW i3, Renault ZOE, Ford Focus Electric, Nissan Leaf and Kia Soul [23] [24] [25] [26]
122 [27].

123 In the last few years EVs are becoming technologically tempting due to the progress of Lithium-ion
 124 (Li-ion) battery technology that is capable of offering the advantage of higher power, as well as higher
 125 energy density. Given that Li-ion batteries are generally preferred as the main power source of the current
 126 EVs [28], in the present study it is implicitly considered that EVs in this case-study employ such type of
 127 batteries. In fact, virtually all EVs that are available in the market today use this battery type due to its
 128 mature technology. The battery capacity for light vehicles in EVs is in the range of 6 kWh to 35 kWh.
 129 The charging time varies from 14 hours for slow charging batteries to less than an hour for fast charging
 130 batteries [29].

131 All the EVs considered in this study employ Li-ion batteries and to understand better effect of
 132 charging on the daily baseline load profile, the charging behaviour of a Li-ion battery is briefly described.
 133 While the SOC of the battery is low, then the charger functions at rated current, therefore it allows a great
 134 quantity of the battery SOC being re-established in the course of the initial charging hours. In practice, the
 135 process of charging a Li-ion battery, despite being represented by simplified characteristics, is described
 136 by a relation that reflects the mutually dependent occurrences of battery SOC and charger type [30]. The
 137 process pursues until the limit of the battery voltage is reached, at which the current falls while the EV
 138 charger preserves a constant voltage. The EV battery charging process is assumed to be continuous as
 139 soon as it is initiated until the full capacity of the battery is reached.

140 *2.2 Model of EV Charging Load*

141 In this paper and for both case studies the charging profile of Li-ion EV batteries is utilized, and the
 142 stochastic behaviour of the EV battery SOC at the starting point of the charging process is calculated
 143 using a probability density function (PDF) associated with the driving range as in [19] [31]. The EV
 144 charging demand is given by the initial battery SOC, the charging start time and characteristics. Travel
 145 habits of the EV before the recharging process define the SOC at the beginning of the charging process of
 146 an EV battery and can be perceived as a random variable associated to the driving range. Using as a basis
 147 a study on the general travel information regarding Portuguese drivers of conventional vehicles recorded
 148 in 2011 in Lisbon area [32], a PDF of day-to-day driving range can be constructed as expressed by (1):

$$149 \quad (d; \mu, \sigma) = \frac{1}{d\sqrt{2\pi\sigma^2}} \times e^{-\frac{(\ln d - \mu)^2}{2\sigma^2}}, \quad d > 0 \quad (1)$$

150 By knowing the average daily driving range, the SOC at the beginning of a recharge cycle, that is the
 151 residual battery capacity, is calculated utilizing (2), assuming that each trip is initiated with 100% SOC
 152 and that the SOC descends linearly during the course of the journey (2):

$$153 \quad E_i = \left(1 - \frac{d}{d_R}\right) \times 100 \% \quad (2)$$

154 A typical average value for travel distance is 100 km [33].

155 By replacing (2) into (1) and switching the variable from d to E , and by succeeding the journey of one
 156 day, the PDF of the SOC of the battery is expressed as follows (3):

$$157 \quad h(E; \mu, \sigma) = \frac{1}{d_R(1-E)\sqrt{2\pi\sigma^2}} \times e^{-\frac{[\ln(1-E) - (\mu - \ln d_R)]^2}{2\sigma^2}}, \quad 0 < E < 1 \quad (3)$$

158 The PDF is truncated between 25% and 95% of battery SOC with parameters as in [34]. Since the
 159 equation is truncated at 25% and 95% of battery SOC it means that at the beginning of each charging
 160 process the battery can range from 25% to 95% of SOC depending on the travel habits of EV users.
 161 Consequently, EVs that are at, for example, 92% SOC – charge within minutes while the ones that are at,
 162 for instance, 26% will take hours to reach the full charge in the slow charging mode.

163 Based on the information drawn from both PDF, it is possible to estimate the residual battery capacity
 164 at the beginning of a recharge cycle. Both the electricity tariff rate structure and the objective of the use of
 165 the EVs by the users, which is an uncertain factor, influence the initial plug-in instance of the EV and the
 166 battery charging process.

167 *2.3 The Loss of Life of the PDT*

168 Since the PDT is a vital part of the DN, a proper conservation of mineral-oil-tilled PDTs is of a high
 169 importance in power systems and therefore, the necessity of implementing a caring methodology
 170 concerning PDT loading emerges [35].

171 The PDT insulation system is essentially created from paper and oil and both are subject to experience
 172 deterioration. Load intensification has an effect on the increase of the Θ_h and subsequently the thermal
 173 deterioration of the paper is affected [36] [37] [38].

174 As the distribution of the temperature is uneven, the most deteriorated section of the PDT will be the
 175 one with the highest temperature [39]. Thus, the Θ_h temperature directly affects the life duration of PDTs
 176 [19]. By definition, the Θ_h is the highest temperature of any spot in the PDT winding. By experiencing

177 elevated electrical loads it originates high core-winding temperatures which in turn cause chemical
 178 breakdown of insulating oil and insulating paper [36] [37].

179 2.3.1 Assessment of Θ_h temperature through exponential equations

180 In the case of ever-increasing steps of loads, Θ_o and winding Θ_h rise until a step equivalent to load
 181 factor K . As a consequence, equation of the top-oil $\Theta_o(t)$ temperature is shown in the following
 182 expression (4):

$$183 \quad \Theta_o(t) = \Delta\Theta_{oi} + \left\{ \Delta\Theta_{or} \times \left[\frac{1+R \times K^2}{1+R} \right]^x - \Delta\Theta_{oi} \right\} \times \left(1 - e^{-t/(k_{11} \times \tau_o)} \right) \quad (4)$$

184 The hot-spot temperature rise $\Delta\Theta_h(t)$ is as follows (5):

$$185 \quad \Delta\Theta_h(t) = \Delta\Theta_{hi} + \left\{ H \times g_r \times K^y - \Delta\Theta_{hi} \right\} \times \left[k_{21} \times \left(1 - e^{-t/(k_{22} \times \tau_w)} \right) - (k_{21} - 1) \times \left(1 - e^{-t \times k_{22} / \tau_o} \right) \right] \quad (5)$$

186 For decreasing step of loads situations, the Θ_o and winding Θ_h are reduced until a step corresponding to
 187 a K [36]. The equation of the top-oil temperature $\Theta_o(t)$ is expressed as following (6):

$$188 \quad \Theta_o(t) = \Delta\Theta_{or} \times \left[\frac{1+R \times K^2}{1+R} \right]^x + \left\{ \Delta\Theta_{oi} - \Delta\Theta_{or} \times \left[\frac{1+R \times K^2}{1+R} \right]^x \right\} \times \left(e^{-t/(k_{11} \times \tau_o)} \right) \quad (6)$$

189 The Θ_h increase is set by (7):

$$190 \quad \Delta\Theta_h(t) = H \times g_r \times K^y \quad (7)$$

191 In conclusion, by taking into consideration $\Theta_o(t)$ and $\Delta\Theta_h(t)$ from (4) and (5) in case of increasing load
 192 steps, and (6) and (7) in case of decreasing load steps and by taking into account the ambient temperature
 193 Θ_a the complete hot-spot temperature $\Theta_h(t)$ expression is estimated as follows (8):

$$194 \quad \Theta_h(t) = \Theta_a + \Theta_o(t) + \Delta\Theta_h(t) \quad (8)$$

195 2.3.2 Assessment of Θ_h temperature through differential equations

196 When heat-transfer principles are applied to the PDT situation, the differential equations for Θ_o (inputs
 197 K , Θ_a and output Θ_o) is:

$$198 \quad \left[\frac{1+K^2R}{1+R} \right]^x \times (\Delta\Theta_{or}) = k_{11} \tau_o \times \frac{d\Theta_o}{dt} + [\Theta_o - \Theta_a] \quad (9)$$

199 The differential equation for Θ_h rise (inputs K and output $\Delta\Theta_h$) is most easily solved as the sum of two
 200 differential equations where:

201
$$\Delta\Theta_h = \Delta\Theta_{h1} - \Delta\Theta_{h2} \quad (10)$$

202 The two equations are:

203
$$k_{21} \times K^y \times (\Delta\Theta_{hr}) = k_{22} \times \tau_w \times \frac{d\Delta\Theta_{h1}}{dt} + \Delta\Theta_{h1} \quad (11)$$

204 and

205
$$(k_{21} - 1) \times K^y \times (\Delta\Theta_{hr}) = \left(\frac{\tau_o}{k_{22}}\right) \times \frac{d\Delta\Theta_{h2}}{dt} + \Delta\Theta_{h2} \quad (12)$$

206 the solutions of which are combined in accordance with equation (8). The final equation for the Θ_h is:

207
$$\Theta_h = \Theta_o + \Delta\Theta_h \quad (13)$$

208 If the differential equations are converted to difference equations, then the solution is quite
 209 straightforward, even on a simple spreadsheet. The differential equations (7-11) can be written as the
 210 following difference equations, where D stands for a difference over a small time step. Equation (7)
 211 becomes:

212
$$D\Theta_o = \frac{Dt}{k_{11}\tau_o} \left[\left[\frac{1+K^2R}{1+R} \right]^x \times (\Delta\Theta_{or}) - [\Theta_o - \Theta_a] \right] \quad (14)$$

213 The D operator implies a difference in the associated variable that corresponds to each time step Dt . At
 214 each time step, the n th value of $D\Theta_o$ is calculated from the $(n-1)$ th value using:

215
$$\Theta_{o(n)} = \Theta_{o(n-1)} + D\Theta_{o(n)} \quad (15)$$

216 Equations (9) and (10) become:

217
$$D\Delta\Theta_{h1} = \frac{Dt}{k_{22}\tau_w} \times [k_{21} \times \Delta\Theta_{hr} K^y - \Delta\Theta_{h1}] \quad (16)$$

218 and

219
$$D\Delta\Theta_{h2} = \frac{Dt}{\frac{1}{k_{22}}\tau_o} \times [(k_{21} - 1) \times \Delta\Theta_{hr} K^y - \Delta\Theta_{h2}] \quad (17)$$

220 The n^{th} values of each of $\Delta\Theta_{h1}$ and $\Delta\Theta_{h2}$ are calculated in a way similar to equation (13). The total Θ_h
 221 rise at the n^{th} time step is given by:

222
$$\Delta\Theta_{h(n)} = \Delta\Theta_{h1(n)} + \Delta\Theta_{h2(n)} \quad (18)$$

223 Finally, the Θ_h temperature at the n th time step is given by:

224
$$\Theta_{h(n)} = \Theta_{o(n)} + \Delta\Theta_{h(n)} \quad (19)$$

225 *2.3.3 The PDT calculation of loss of life.*

226 In case of the thermally upgraded paper the equation of the ageing rate V is expressed as follows [37]:

$$227 \quad V = e^{\left(\frac{15000}{110+273} - \frac{15000}{\theta_h+273} \right)} \quad (20)$$

228 The ageing rate V [40] corresponds to the deterioration of paper insulation at a temperature Θ_h which is
 229 higher or lower than 110°C, with respect to the ageing rate at 110°C [36]. The loss of life (LOL) of
 230 cellulose insulation which calculated using the differential equations can also be expressed with
 231 difference equations. The fundamental differential equation is:

$$232 \quad \frac{dL}{dt} = V \quad (21)$$

233 implying:

$$234 \quad DL_{(n)} = V_{(n)} \times Dt \quad (22)$$

235 and:

$$236 \quad L_{(n)} = L_{(n-1)} + DL_{(n)} \quad (23)$$

237 The LOL equation L can also be rewritten and for the duration of the time segment t_n is expressed as
 238 following:

$$239 \quad L = \int_{t_1}^{t_2} V dt \quad \text{or} \quad L \approx \sum_{n=1}^N V_n \times t_n \quad (24)$$

240 **3. Simulation Results**

241 *3.1 The PDT Properties*

242 In order to determine transient solutions for Θ_o and Θ_h a thermal model is developed and proposed for
 243 the PDT and can be applied to both three-phase and to single-phase PDTs.

244 The PDT power rating and cooling system is provided by the insular DSO. The properties of both
 245 PDTs used in this paper are obtained from Ravetta et al. [41] that presented the data of a real 250 and 630
 246 kVA (P_r) oil PDTs with Oil Natural Air Natural (ONAN) cooling where a natural convectional flow of
 247 hot oil is utilized for cooling. The constants are taken from [36]. Both PDTs properties are drawn from
 248 [42] and [43].

249 *3.2 Structural elements of the insular grid*

250 The Azores are a Portuguese autonomous region and a 9 islands archipelago located in the North
 251 Atlantic, circa 3900 km from the east coast of North America. São Miguel Island is the capital and most

252 populated island. The island has around 140,000 inhabitants and covers an area of 760 km². In this paper,
253 a part of São Miguel medium voltage DN is investigated.

254 The research portrayed in this paper focuses on two different cases in which the evaluation of the
255 effect of EVs charging loads on the dielectric oil deterioration of two real oil-immersed PDTs, one
256 supplying a residential area and the other a private industrial client, which are referred to as case study 1
257 and 2, respectively. The EVs starting time of charging is selected by taking into account the daily habits of
258 São Miguel's people and the off-peak tariff. In this regard, data are provided under SiNGULAR project
259 [44].

260 Two different percentages of EVs are used for the two different cases under investigation. The
261 percentage of BMW i3 was chosen in both case studies as high as 40% since it is the fastest selling EV in
262 Portugal according to the Portuguese Automobile Association (Associação Automóvel de Portugal –
263 ACAP) [45]. Renault ZOE and Ford were selected to have a 20% market penetration since these brands
264 already appear to have a significant share in the conventional vehicle market [45]. Data for the charging
265 types and duration of the five EVs are presented in [42] for the first case study and for [43] the second
266 case study.

267 The present market outlook of EVs can be considered globally low, not exceeding a 7% share in
268 leading countries such as Norway [19]. On the other hand, in this paper, very high penetration levels are
269 examined. Particularly for an insular area, such as São Miguel, the relatively high transportation cost of
270 fossil fuels, the presence of rich potential of RES, and the opportunities that emerge from the efficient
271 management of an EV fleet [13], are factors that have led the authors to believe that the penetration levels
272 that are likely to be met in such areas in the future will be significantly higher than in continental areas. In
273 addition, supporting initiatives made by governments frequently have a tendency to aim specific areas
274 such as islands and as a result, potential funding programs or tax reduction schemes to endorse the
275 acquisition and use of EVs are highly expected to significantly encourage customers to exchange their
276 fossil-fuelled internal combustion engine vehicles with EVs [46].

277 *3.3 Case Study 1*

278 For this case study a PDT that supplies a residential area is chosen. The part of the medium voltage DN
279 and an identification of several outputs are withdrawn and can be seen in [42]. For this case study the

280 PDT substation PT80 which supplies 292 households through a 630kVA, 10kV/0.4kV oil-immersed PDT
 281 is used.

282 During the summer of 2014 a number of measurements were performed at the PDT substation PT80
 283 and the energy consumption of 292 households was collected. Plus, the daily temperature records were
 284 made for the aforementioned period as shown in Fig. 1. The baseline load profile is withdrawn from [42].
 285 It may be observed that a 630 kVA PDT is oversized for a 140 kW of peak in daily baseline load profile,
 286 even if in Azores higher consumption is witnessed during the summer [21].

287 "Figure 1 can be observed at the end of the document".

288 The EV load demand can be affected to some extent by the electricity tariff structure. For this model
 289 the current electricity tariff of Azores Islands that entered into force in 2015 is taken into account. Even
 290 though a three rate tariff for domestic consumers currently exists in Azores, for this study the two rate
 291 tariff is used. The off-peak tariff is 190% lower than the peak tariff and it is initiated instantly after 22:00
 292 [47].

293 Based on the data collected from the PDF it is possible to apply the PDT thermal model, using the load
 294 ratio as an input to obtain the Θ_h and Θ_o . For this case study one day and a half of the baseline load profile
 295 of the summer period of the PDT substation PT80 is used.

296 The total load (in kW) on the PDT is the summation of the n_d domestic loads P_d and loading from n_{EV}
 297 randomly selected EVs:

$$298 \quad P(t) = \left| n_d P_d(t) + \sum_{EV=1}^{n_{EV}} P_{EV}(t) \right| \quad (25)$$

299 A fitting algorithm is applied to assess the impact of EVs charging loads on the dielectric oil
 300 deterioration of PDT based on the previously presented methodology. Battery charging of the electric
 301 vehicles inflicts an extra load on the PDT. By hypothesizing that a PDT supplies several EVs in a
 302 neighbourhood, different charging time and load profiles are obtained for the PDT. The algorithm
 303 integrates data obtained from the PDF and calculates the Θ_h and the PDT LOL due to EVs charging loads.

304 Two different scenarios are studied, the first being with different initial SOC of the EVs based on the
 305 PDF function, plus different penetration ratios of EVs are considered in this study for the household
 306 neighbourhood, beginning with 75% penetration and then with 80%, 85%, 90%, 95% and 100%. Also, it
 307 is considered that 50% of the EV owners charge their cars in slow charging mode and the other 50% in

308 domestic fast charging mode since the model can be applied for both. Finally, it is assumed that 55% of
309 EVs begin charging at 22:00 or are scheduled to do so since as seen before, for Azores the off-peak tariff
310 is 190% lower than peak tariff and it becomes available exactly at 22:00 of each day, as for the remaining
311 45% of EVs, it is assumed that these users are not very concerned with off-peak tariffs and that the EVs
312 charging are set to begin at 07:00 or are scheduled to do so, when users wake up and go to work and the
313 slow charging mode is used after home arrival, usually after 18:00. These specific percentages are chosen
314 as such due to the reason of being just under and/or above the PDT loading limit, other percentages are
315 redundant.

316 The second scenario explores a case where during the weekend and at the rule of the same off-peak
317 tariff all the EVs are scheduled or the users chose to charge or the EVs are set to charge at 22:00 and all
318 the owners charge their cars in slow charging mode. The impact on the daily baseline load profile of the
319 PDT substation PT80 made by the energy consumption of the EVs at several penetration ratios from both
320 scenarios is shown in Fig. 2 and in Fig. 4, respectively, where (hh:mm) signifies the time in hours and
321 minutes. The starting times of charging for the first scenario is chosen due to the fact that EV users
322 typically do not have a need for fast recharging since they dispose of sufficient time - 3 to 8 h (depending
323 on the charge level) during the non-working period of the day or after 22:00 at the residence with the
324 intention of skipping the drawback of recurring to a public charging station.

325 By analysing Figs. 2 and 4 it can be concluded that for a penetration of EVs of more than 75% the PDT
326 is overloaded. It is then possible to assess the PDT insulation ageing affected by the Θ_h and the LOL of
327 the PDT which is presented in Figs. 3 and 5, respectively.

328 "Figure 2 can be observed at the end of the document".

329 "Figure 3 can be observed at the end of the document".

330 "Figure 4 can be observed at the end of the document".

331 "Figure 5 can be observed at the end of the document".

332 Using the ageing equations (20) and (24), the LOL of the PDT can now be determined. The LOL of the
333 PDT is presented in percentage and also in hours and minutes for each day of EV charging which means
334 that from the PDT expected life at 0% penetration (180000 hours) is withdrawn a number of hours for
335 each day of charging. The results can be seen the Table 1.

336 "Table 1 can be observed at the end of the document".

337 From Fig. 2 to 5 and from the Table 1 it can be concluded that the off-peak tariff will encourage users
 338 to prefer a certain hour of charging, in this case, 22:00, that will cause a concentration of EVs charging at
 339 the same time which in turn will generate an overloading of the PDT, a sudden increase of the Θ_h and
 340 consequently will affect the PDT lifetime.

341 In both scenarios it can be concluded that for more than 75% of EV penetration the PDT will
 342 overloaded resulting in a growth of the Θ_h of the PDT. The LOL increases with the increase of EV
 343 penetration in both scenarios.

344 By analysing the results obtained from Table 1 it can be concluded that the PDT LOL is only affected
 345 after a certain amount of EV penetration which is relatively high. If the EV users keep this profile of
 346 charging every day the PDT will have a deteriorating LOL after some time.

347 3.4 Case Study 2

348 This case focuses on a PDT that supplies a private industrial client. A part of the medium voltage DN
 349 and an identification of several outputs and can be seen in [43].

350 In this case study the PDT substation PT1094 is used which supplies one private industrial client
 351 through a 250kVA, 10kV/0.4kV oil-immersed PDT.

352 The private industrial client consists of a factory that produces sugar out of sugar beet. It employs 120
 353 workers and operates in 3 working shifts of 8 hours each. The first working shift starts at 08:00, the
 354 second at 16:00 and the third at 00:00. It is assumed in this paper that the workers are evenly distributed
 355 throughout the working shifts.

356 During the summer of 2014 several measurements were made at the PDT substation PT1094 and the
 357 energy consumption of industrial client was recorded and as a consequence a daily baseline load profile is
 358 generated and can be observed in [43]. It is also given the power factor of the PDT – approximately 0.95.
 359 It may be observed that a 250 kVA PDT is properly sized for a 140 kW of peak in daily baseline load
 360 profile, considering that a typical value for an inferior size PDT would be 167 kVA which is not
 361 satisfactory [21].

362 The total load $P(t)$ (in kW) on the PDT is the sum of the factory load $P_f(t)$ and loading from n_{EV}
 363 randomly selected EVs:

$$364 \quad P(t) = \left| P_f(t) + \sum_{EV=1}^{n_{EV}} P_{EV}(t) \right| \quad (26)$$

365 For this case study one day of the baseline load profile of the summer period of the PDT substation
366 PT1094 is used and two different scenarios are examined.

367 *3.4.1 Scenario 1*

368 For the first scenario different penetration ratios of EVs for each working shift are considered for this
369 industrial client, beginning with 35% penetration and then with 40%, 45%, 50%, and 55 %. The number
370 of EVs in this case can be calculated simply by dividing the 120 employees by 3 shifts, resulting in 40
371 workers per shift. Thus, for instance, 50% of EVs translates in 20 EVs charging per shift. These specific
372 percentages are chosen as such due to the reason of being just under and/or above the PDT loading limit,
373 other percentages are redundant. Finally it is assumed that the EVs start or are scheduled to charge at the
374 beginning of each working shift.

375 The effect on the daily baseline load profile of the PDT substation PT1094 created by the energy
376 consumption of the EVs at several penetration ratios from the first scenario is shown in Fig. 6. The daily
377 baseline load profile is also shown as 0% penetration ratio.

378 By analysing Fig. 6 it can be observed that for a penetration of EVs of more than 40% the PDT is
379 overloaded. Also, from the information obtained from the model and presented in Fig. 6, it is possible to
380 assess the PDT insulation ageing affected by the Θ_h which is presented in Fig. 7 and subsequently to
381 calculate LOL at the designated penetration ratios of the PDT. The LOL of the PDT is presented in
382 percentage and in hours and minutes for each day of EV charging which means that from the PDT
383 expected life at 0% penetration is subtracted the number of minutes or hours for each day of charging.
384 The results can be seen in the Table 2.

385 "Figure 6 can be observed at the end of the document".

386 "Figure 7 can be observed at the end of the document".

387 "Table 2 can be observed at the end of the document".

388 *3.4.2 Scenario 2*

389 The second scenario is as follows: all EVs are charged with fast charging mode beginning with 15%
390 penetration and then with 20%, 25%, 30%, and 35%. The same percentages are set as the preceding
391 scenario in order to observe the difference between slow and fast charging modes. Just as in the previous
392 scenario, it is assumed that the workers put their EVs to charge at the beginning of each working shift.

393 The consequence on the daily baseline load profile of the PDT substation PT1094 made by the energy
394 consumption of the EVs at several penetration ratios from the second scenario is shown in Fig. 8.

395 By observing Fig. 8 it can be noticed that for a penetration of EVs of more than 15% the PDT is
396 profoundly overloaded and even at inferior penetration ratios it is overloaded. Also, from the information
397 obtained from the model and presented in Fig. 8, it can be assessed the PDT insulation ageing affected by
398 the Θ_h which is presented in Fig. 9. By means of the ageing equations (5) and (6), the LOL of the PDT
399 can now be determined. The results can also be seen in the Table 2.

400 "Figure 8 can be observed at the end of the document".

401 "Figure 9 can be observed at the end of the document".

402 *3.4.3 Critical Analysis*

403 By analysing the results obtained from Table 2 it can be concluded that the PDT LOL is only affected
404 after a certain amount of EV penetration which is relatively high. If the EV users make such profile of
405 charging a routine the PDT will have a deteriorating LOL after some time.

406 The comparison of both scenarios at 35% EV penetration in the Figs. 10 and 11 highlights the level of
407 impact in the PDT ageing by using fast charging over slow charging. By analysing Figs. 6 to 9 and Table
408 2 it can be concluded that each beginning of a shift will influence users to prefer the first hour of
409 charging, that will originate a concentration of EVs charging at the same time which in turn could cause
410 an overloading of the PDT, a sudden increase of the Θ_h and thus will affect the PDT lifetime.

411 "Figure 10 can be observed at the end of the document".

412 "Figure 11 can be observed at the end of the document".

413 By observing the first scenario it can be concluded that for more than 40% of EV penetration the PDT
414 will be overloaded resulting in an increase of the Θ_h of the PDT. The LOL slightly increases with the
415 increase of EV penetration in this scenario.

416 In an improbable event of the second scenario occurring, the LOL of the distribution PDT is
417 significantly higher. Thus, it is advised to avoid the fast charging mode since the slow mode takes at
418 maximum 5 hours which is always less than a working shift of 8 hours.

419

420

421

422 **4. Conclusions** 423

424 In this paper a model to estimate the influence of simultaneous EVs charging on the dielectric oil
425 deterioration of two PDTs, one at a residential area and other at a private industrial client, was applied.
426 Two different case studies were examined, one focusing on a residential area during working days and
427 weekends and another concerning a private industrial client with several penetration ratios at three
428 different working shifts. The power rating of both PDTs and the cooling system were provided by the
429 local DSO. Since the PDT insulation ageing is mainly affected by the Θ_h and by knowing the load ratio a
430 PDT thermal model was utilized to calculate the Θ_h . The main inputs to the model, including residential
431 load, PDT parameters, and five different vehicle parameters were taken from real data. Dielectric oil
432 deterioration was then calculated and analysed. Since both PDTs have a significant capacity to be used for
433 a side activity – this study shows that even though it has, it still can be overloaded after a specific increase
434 of EV penetration. The developed methodology was applied to assess the impact of multiple EVs
435 charging in the same residential area and it showed that off peak tariff can have an influence over EV
436 users and affect the PDT lifetime. The results show that the LOL of the PDT is only affected after a
437 certain amount of EV penetration, which is relatively high. In both case studies the penetration ratios that
438 reach the limit of the transformer were studied; thus, if the penetration of the EVs increase from these
439 scenarios onward then a more accelerating deterioration of the oil is expected. The second case study
440 showed also that while charging at the workplace, the slow charging mode was recommended over the
441 fast mode. Even if the slow charging mode was selected by the users the vehicles will always be 100%
442 charged at the end of each working shift and without drastically affecting the PDT lifetime when
443 compared to the fast charging mode.

444

445 **Acknowledgements**

446 This work was supported by FEDER funds (European Union) through COMPETE and by Portuguese
447 funds through FCT, under FCOMP-01-0124-FEDER-020282 (Ref. PTDC/EEA-EEL/118519/2010),
448 UID/CEC/50021/2013 and SFRH/BPD/103744/2014. The research leading to these results has also
449 received funding from the EU Seventh Framework Programme FP7/2007-2013 under grant agreement no.
450 309048.

451 **References**
452

- [1] A. Hackbarth and R. Madlener, "Willingness-to-pay for alternative fuel vehicle characteristics: A stated choice study for Germany," *Transportation Research Part A: Policy and Practice*, vol. 85, pp. 89-111, 2016.
- [2] H. Morais, T. Sousa, J. Soares, P. Faria and Z. Vale, "Distributed energy resources management using plug-in hybrid electric vehicles as a fuel-shifting demand response resource," *Energy Conversion and Management*, vol. 97, pp. 78-93, 2015.
- [3] J. P. Torreglosa, P. García-Triviño, L. M. Fernández-Ramirez and F. Jurado, "Decentralized energy management strategy based on predictive controllers for a medium voltage direct current photovoltaic electric vehicle charging station," *Energy Conversion and Management*, vol. 108, pp. 1-13, 2016.
- [4] P. Jochem, S. Babrowski and W. Fichtner, "Assessing CO2 emissions of electric vehicles in Germany in 2030," *Transportation Research Part A: Policy and Practice*, vol. 78, pp. 68-83, 2015.
- [5] A. Schuller, "Charging Coordination Paradigms of Electric Vehicles," in *Plug In Electric Vehicles in Smart Grids*, Singapore, Springer, 2015, pp. 1-21.
- [6] A. Khazali and M. Kalantar, "A stochastic-probabilistic energy and reserve market clearing scheme for smart power systems with plug-in electrical vehicles," *Energy Conversion and Management*, vol. 105, pp. 1046-1058, 2015.
- [7] Z. Duan, B. Gutierrez and L. Wang, "Forecasting Plug-In Electric Vehicle Sales and the Diurnal Recharging Load Curve," *IEEE Transactions on Smart Grid*, vol. 5, no. 1, pp. 527-535, 2014.
- [8] P. Richardson, D. Flynn and A. Keane, "Optimal Charging of Electric Vehicles in Low-Voltage Distribution Systems," *IEEE Transactions on Power Systems*, vol. 27, no. 1, pp. 268-279, 2012.
- [9] A. M. Haidar, K. M. Muttaqi and D. Sutanto, "Technical challenges for electric power industries due to grid-integrated electric vehicles in low voltage distributions: A review," *Energy Conversion and Management*, vol. 86, p. 689-700, 2014.
- [10] R. Das, K. Thirugnanam, P. Kumar, R. Lavudiya and M. Singh, "Mathematical Modeling for Economic Evaluation of Electric Vehicle to Smart Grid Interaction," *IEEE Transactions on Smart Grid*, vol. 5, no. 2, pp. 712-721, 2014.
- [11] H. Shayeghi, A. Ghasemi, M. Moradzadeh and M. Nooshyar, "Simultaneous day-ahead forecasting of electricity price and load in smart grids," *Energy Conversion and Management*, vol. 95, pp. 371-384, 2015.
- [12] F. H. Malik and M. Lehtonen, "A review: Agents in smart grids," *Electric Power Systems Research*, vol. 131, pp. 71-79, 2016.
- [13] O. Erdinc, J. Catalao, M. Uzunoglu and A. Rifat Boynuegri, "Smart insular grids: Opportunities and challenges," in *2013 3rd International Conference on Electric Power and Energy Conversion Systems (EPECS)*, Istanbul, 2013.
- [14] S. Jazebi, S. Hosseinian and B. Vahidi, "DSTATCOM allocation in distribution networks considering reconfiguration using differential evolution algorithm," *Energy Conversion and Management*, vol. 52, no. 7, pp. 2777-2783, 2011.
- [15] J. Sexauer, K. McBee and K. Bloch, "Applications of probability model to analyze the effects of electric vehicle chargers on distribution transformers," *IEEE Transactions on Power Systems*, vol. 28, no. 2, pp. 847-854, 2015.
- [16] Q. Gong, S. Midlam-Mohler, V. Marano and G. Rizzoni, "Study of PEV Charging on Residential Distribution Transformer Life," *IEEE Transactions on Smart Grid*, vol. 3, no. 1, pp. 404-412, 2012.
- [17] A. Hilshey, P. Hines, P. Rezaei and J. Dowds, "Estimating the Impact of Electric Vehicle Smart Charging on Distribution Transformer Aging," *IEEE Transactions on Smart Grid*, vol. 4, no. 2, pp. 905-913, 2013.
- [18] R. Vicini, O. Micheloud, H. Kumar and A. Kwasinski, "Transformer and home energy management systems to lessen electrical vehicle impact on the grid," *IET Generation, Transmission & Distribution*, vol. 6, no. 12, pp. 1202-1208, 2012.
- [19] K. Qian, C. Zhou and Y. Yuan, "Impacts of high penetration level of fully electric vehicles charging loads on the thermal ageing of power transformers," *International Journal of Electrical Power & Energy Systems*, vol. 65, pp. 102-112, 2015.

- [20] Q. Gong, S. Midlam-Mohler, E. Serra, V. Marano and G. Rizzoni, "PEV Charging Control Considering Transformer Life and Experimental Validation of a 25 kVA Distribution Transformer," *IEEE Transactions on Smart Grid*, vol. 6, no. 2, pp. 648-656, 2015.
- [21] EDA S.A. - Electricidade dos Açores, "Caracterização Das Redes De Transporte E Distribuição De Energia Eléctrica Da Região Autónoma Dos Açores," Ponta Delgada, 2014.
- [22] K. Young, C. Wang, L. Y. Wang and K. Strunz, "Chapter 2 - Electric Vehicle Battery Technologies," in *Electric Vehicle Integration into Modern Power Networks*, New York, Springer New York, 2013, pp. 15-56.
- [23] Bayerische Motoren Werke, "The new BMW i3 - Launches November 2013.," BMW UK, Printed in the UK, 2013.
- [24] Kia Motors Europe, "The new Kia," Kia Motors Europe, Frankfurt am Main, Germany .
- [25] Renault S.A., "Renault ZOE Simply Revolutionary," Renault U.K. Limited Customer Relations, The Rivers Office Park, Denham Way, Maple Cross, Rickmansworth, Hertfordshire, 2013.
- [26] ©2014 Nissan North America, Inc. , "2014 Nissan Leaf Brochure," Dealer E-Process, 2014.
- [27] Ford Motor Company, "2014 Ford Focus Electric Brochure," Ford Motor Company, 2013.
- [28] S. Castano, L. Gauchia, E. Voncila and J. Sanz, "Dynamical modeling procedure of a Li-ion battery pack suitable for real-time applications," *Energy Conversion and Management*, vol. 92, pp. 396-405, 2015.
- [29] A. Haidar, K. Muttaqi and M. Haque, "Multistage time-variant electric vehicle load modelling for capturing accurate electric vehicle behaviour and electric vehicle impact on electricity distribution grids," *IET Generation, Transmission & Distribution*, vol. 9, no. 16, pp. 2705-2716, 2015.
- [30] F. Pinto, L. Costa, M. F. Dias de Amorini, L. Costa and M. Dias de Amorini, "Modeling spare capacity reuse in EV charging stations based on the Li-ion battery profile," in *2014 International Conference on Connected Vehicles and Expo (ICCVEx)*, Vienna, 2014.
- [31] P. Zhang, K. Qian, C. Zhou, B. Stewart and D. Hepburn, "A Methodology for Optimization of Power Systems Demand Due to Electric Vehicle Charging Load," *IEEE Transactions on Power Systems*, vol. 27, no. 3, pp. 1628-1636, 2012.
- [32] N. B. R. d. C. Pereira, MSc Thesis - Eficiência energética no sector dos transportes rodoviários: metodologia para quantificação do excesso de energia consumida devido ao factor comportamental na condução de veículos automóveis ligeiros, Lisbon: Departamento de Ciências e Tecnologia da Biomassa - Universidade Nova de Lisboa, 2011.
- [33] K. Qian, C. Zhou, M. Allan and Y. Yuan, "Modeling of Load Demand Due to EV Battery Charging in Distribution Systems," *IEEE Transactions on Power Systems*, vol. 26, no. 2, pp. 802-810, 2011.
- [34] S. I. Vagropoulos and A. G. Bakirtzis, "Optimal Bidding Strategy for Electric Vehicle Aggregators in Electricity Markets," *IEEE Transactions on Power Systems*, vol. 28, no. 4, pp. 4031-4041, 2013.
- [35] P. S. Georgilakis, "Environmental cost of distribution transformer losses," *Applied Energy*, vol. 88, no. 9, pp. 3146-3155, 2011.
- [36] IEC 60076-7, "Loading Guide for Oil-immersed Power Transformers," 2005.
- [37] C57.91-2011, "IEEE Guide for Loading Mineral-Oil-Immersed Transformers and Step-Voltage Regulators," IEEE Standard, 2012.
- [38] H. Pezeshki, P. Wolfs and G. Ledwich, "Impact of High PV Penetration on Distribution Transformer Insulation Life," *IEEE Transactions on Power Delivery*, vol. 29, no. 3, pp. 1212-1220, 2014.
- [39] R. Godina, E. M. G. Rodrigues, J. C. O. Matias and J. P. S. Catalão, "Effect of Loads and Other Key Factors on Oil-Transformer Ageing: Sustainability Benefits and Challenges," *Energies*, vol. 8, no. 10, pp. 12147-12186, 2015.
- [40] C57.91-2011, "IEEE Guide for Loading Mineral-Oil-Immersed Transformers and Step-Voltage Regulators," IEEE Standard, 2012.
- [41] C. Ravetta, M. Samanna, A. Stucchi and A. Bossi, "Thermal behavior of distribution transformers in summertime and severe loading conditions," in *19th International Conference on Electricity Distribution*, Vienna, 2007.

- [42] R. Godina, N. Paterakis, O. Erdinc, E. Rodrigues and J. Catalão, “Electric vehicles home charging impact on a distribution transformer in a Portuguese island,” in *2015 International Symposium on Smart Electric Distribution Systems and Technologies — EDST 2015*, Vienna, 2015.
- [43] R. Godina, N. Paterakis, O. Erdinc, E. Rodrigues and J. Catalão, “Impact of EV charging-at-work on an industrial client distribution transformer in a Portuguese island,” in *Proceedings of the 25th Australasian Universities Power Engineering Conference — AUPEC 2015*, Wollongong, 2015.
- [44] SiNGULAR, “Smart and Sustainable Insular Electricity Grids Under Large-Scale Renewable Integration,” Grant Agreement No: 309048, FP7-EU, 2015. [Online]. Available: <http://www.singular-fp7.eu/home/>. [Accessed 2015].
- [45] ACAP, “Associação Automóvel de Portugal,” [Online]. Available: <http://www.acap.pt/pt/home>. [Accessed 20 02 2015].
- [46] O. Erdinc and N. G. Paterakis, “Chapter 1 - Overview of Insular Power Systems: Challenges and Opportunities,” in *Smart and Sustainable Power Systems: Operations, Planning and Economics of Insular Electricity Grids*, Boca Raton, Florida, CRC Press (TAYLOR & FRANCIS Group), 2015, pp. 1-34.
- [47] EDA S.A. - Electricidade dos Açores , “Preçário 2015 das Tarifas da Região Autónoma dos Açores,” EDA - Electricidade dos Açores, Ponta Delgada, 2015.

453
454
455

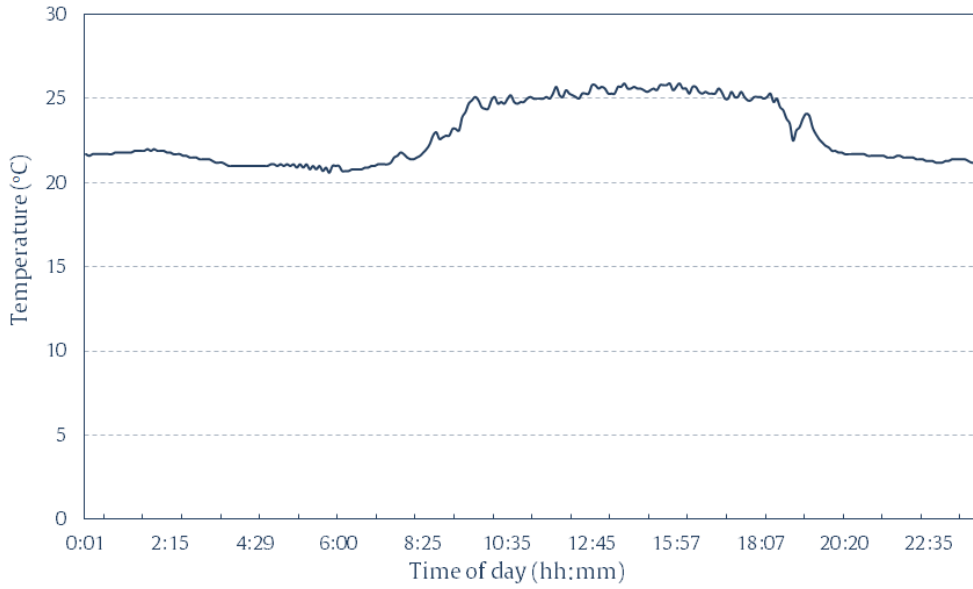


Fig. 1 – Temperature of a typical summer day in São Miguel.

456
457
458
459
460
461

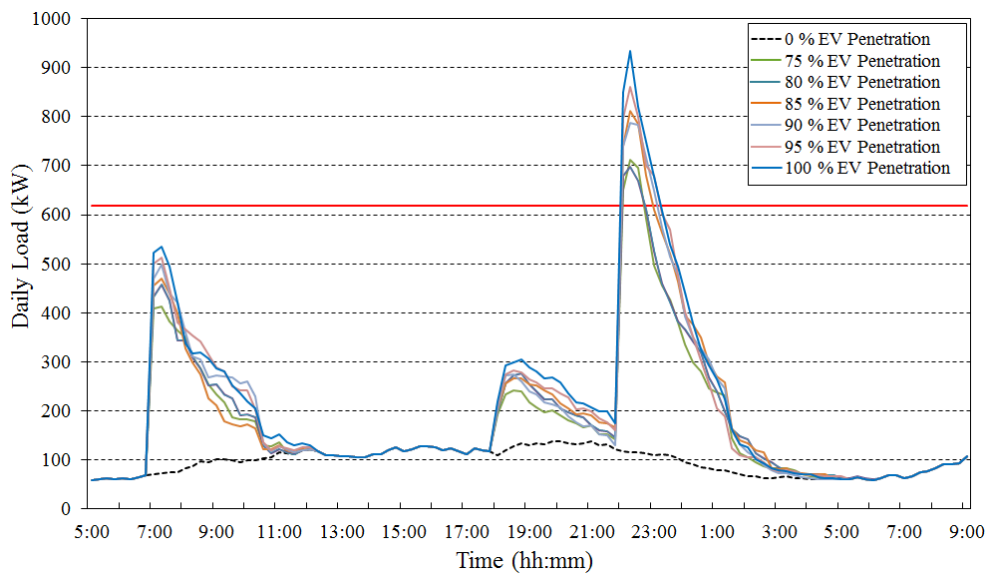
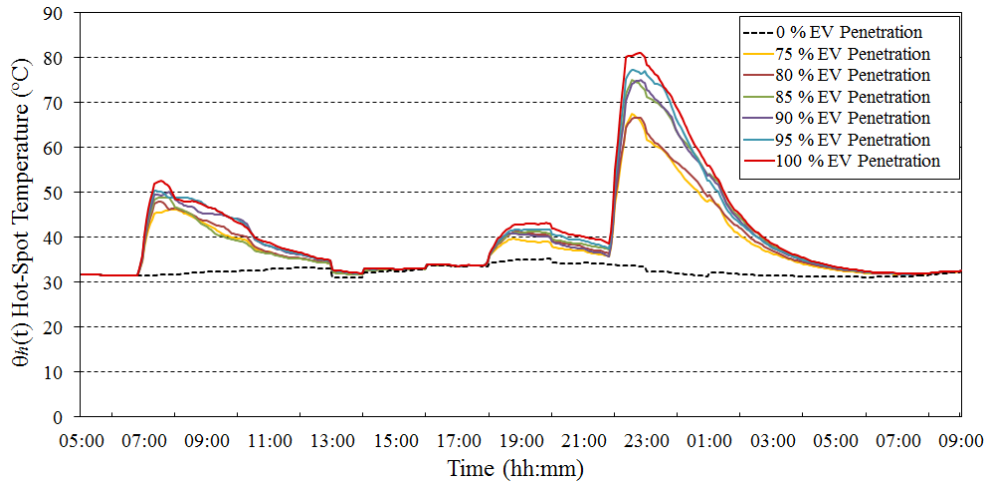


Fig. 2 – The daily baseload profile (case 1, scenario 1).

462
463



464

465

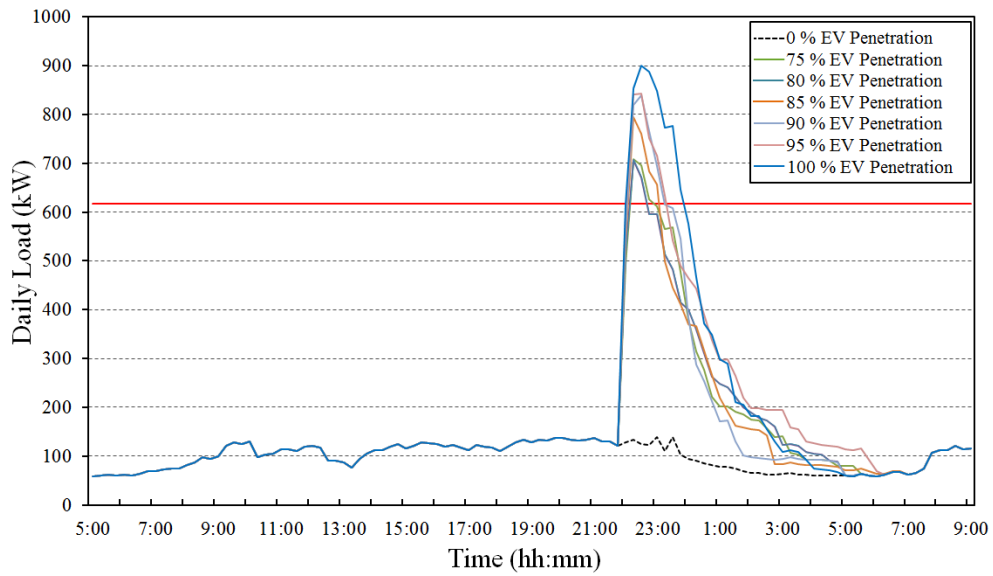
Fig. 3 – The Θ_h of the PDT (case 1, scenario 1).

466

467

468

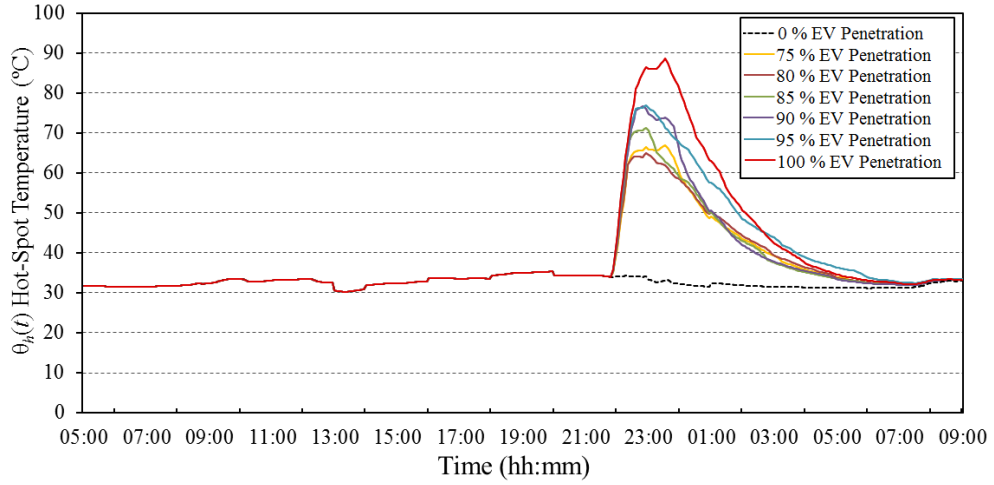
469



470

471

Fig. 4 – The daily baseload profile (case 1, scenario 2).



472

473

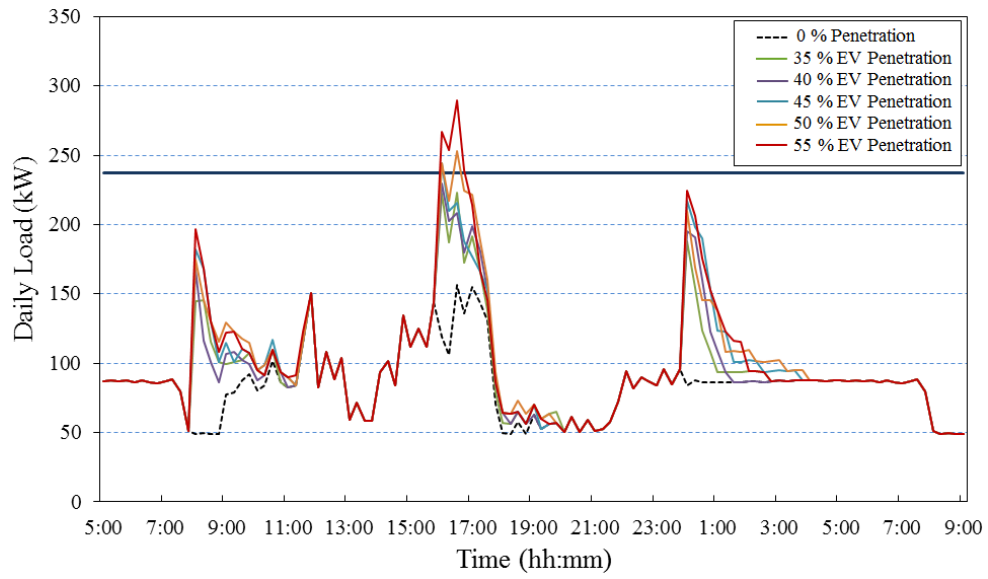
Fig. 5 – The Θ_h of the PDT (case 1, scenario 2).

474

475

476

477

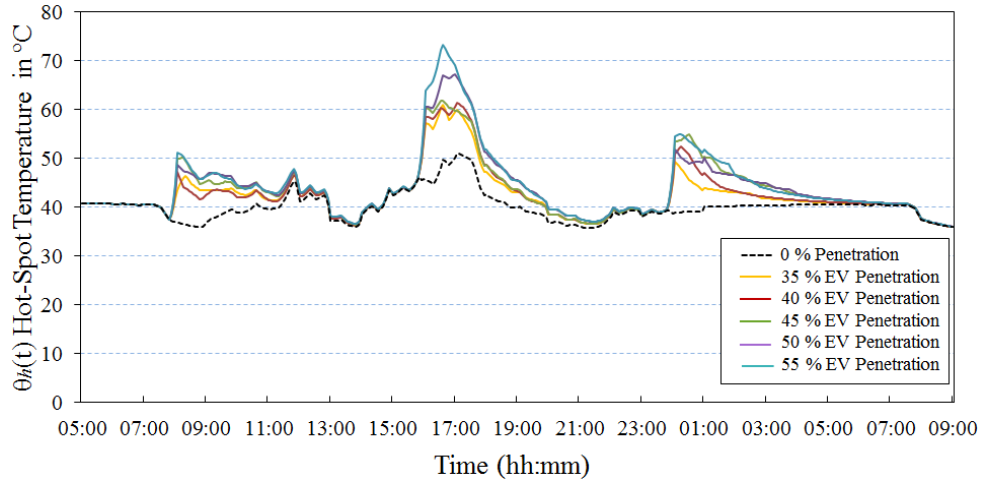


478

479

Fig. 6 – The daily baseload profile (case 2, scenario 1).

480



481

482

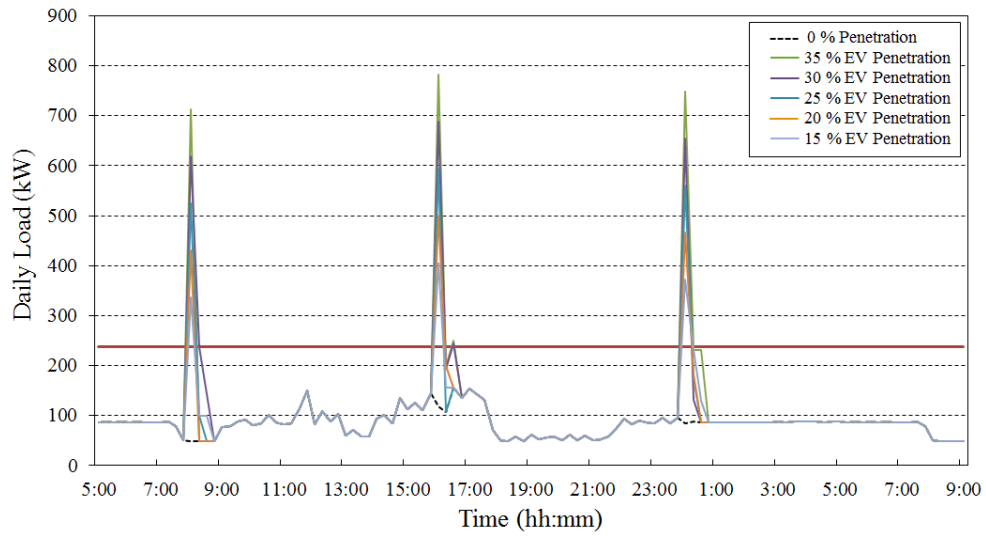
Fig. 7 – The θ_h of the PDT (case 2, scenario 1).

483

484

485

486

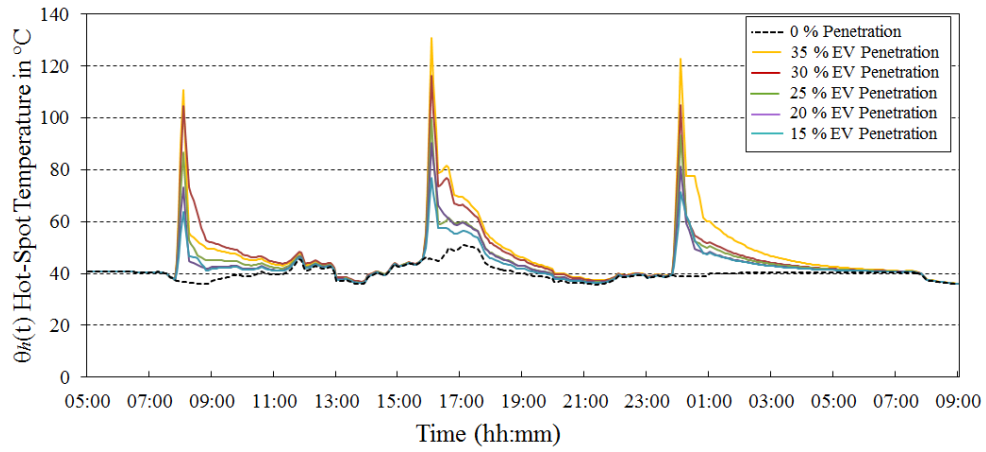


487

488

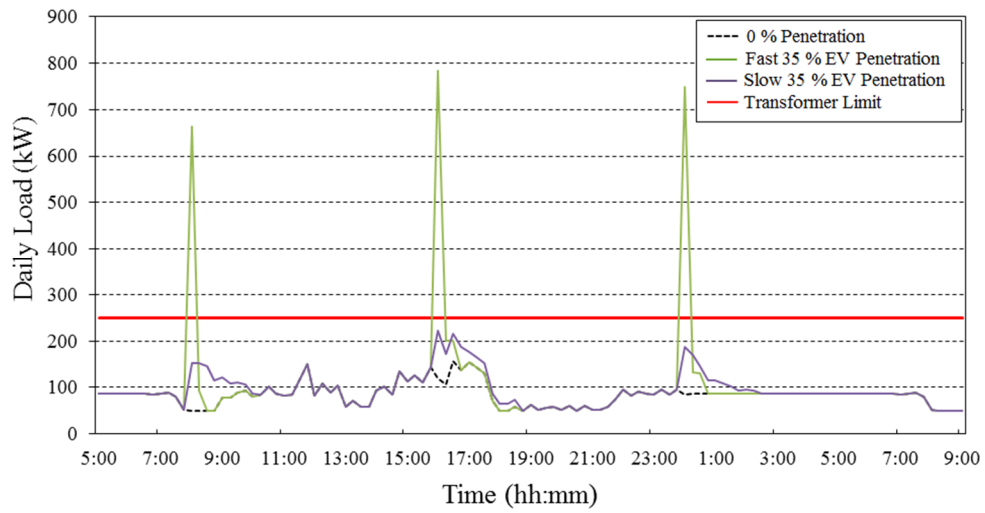
Fig. 8 – The daily baseload profile (case 2, scenario 2).

489



490
491
492
493
494
495

Fig. 9 – The θ_h of the PDT (case 2, scenario 2).



496
497

Fig. 10 – Comparison between scenario 1 and 2 of the daily baseload profile in case 2.

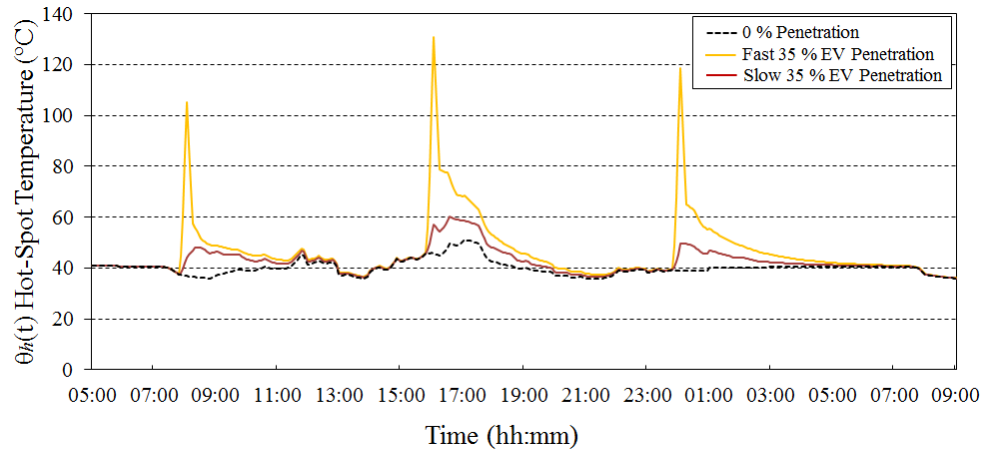


Fig. 11 – Comparison between scenario 1 and 2 of the θ_h of the PDT in case 2.

498

499

500

501

502

503

504

505

506

507

508

509

510

511

512

513

514

515

516

517

518
 519
 520
 521
 522
 523
 524
 525
 526
 527
 528
 529
 530
 531
 532
 533
 534
 535
 536
 537
 538
 539
 540
 541

<i>Level of Penetration</i>	Scenario 1		Scenario 2	
	<i>LOL</i>	<i>% LOL</i>	<i>LOL</i>	<i>% LOL</i>
0%	0h 00m	0	0h 00m	0
75%	0h 50m	0.0005	0h 38m	0.00035
80%	1h 09m	0.0006	0h 46m	0.0004
85%	1h 23m	0.0008	0h 54m	0.0005
90%	1h 41m	0.0009	1h 06m	0.0006
95%	2h 17m	0.0013	1h 24m	0.0008
100%	2h 50m	0.0016	2h 46m	0.0015

Table 1 – Daily transformer LOL due to EV Charging (Case 1)

Scenario 1			Scenario 2		
<i>EV Penetration</i>	<i>LOL (t)</i>	<i>LOL %</i>	<i>EV Penetration</i>	<i>LOL (t)</i>	<i>LOL %</i>
35%	0h 36 min	0.0003	15%	0h 58m	0.0005
40%	0h 40 min	0.0004	20%	1h 22m	0.0004
45%	0h 45 min	0.0004	25%	4h 23m	0.0024
50%	0h 58 min	0.0005	30%	16h 02m	0.0089
55%	0h 77 min	0.0007	35%	70h 22m	0.0391

Table 2 – Daily transformer LOL due to EV charging (Case 2).